https://doi.org/10.5194/gmd-2024-215
Preprint. Discussion started: 25 March 2025

Geoscientific Model Development Discussions

Computation of Self-recruitment in Fish Larvae using Forward- and Backward-in-Time Particle Tracking in a Lagrangian Model (SWIM-v2.0) of the Simulated Circulation of Lake Erie (AEM3D-v1.1.2)

Wei Shi[1], Leon Boegman[1], Josef D. Ackerman[2], Shiliang Shan[1,3], and Yingming Zhao[1,4]
[1]Environmental Fluid Dynamics Laboratory, Department of Civil Engineering, Queen's University, Kingston, ON K7L 3N6, Canada
[2]Physical Ecology Laboratory, Department of Integrative Biology, University of Guelph, Guelph, ON N1G 2W1, Canada
[3]Department of Physics and Space Science, Royal Military College of Canada, Kingston, ON K7K 7B4, Canada
[4]Aquatic Research and Monitoring Section, Ontario Ministry of Natural Resources and Forestry Lake Erie Fishery Station, Wheatley, ON N0P 2P0, Canada

Correspondence to: Wei Shi (weishi.yz@gmail.com)

Abstract. Accurately estimating self-recruitment (SR), the fraction of recruits in a location that originated locally, is critical for understanding population connectivity. Biophysical models have been typically applied to compute SR by releasing a certain number of larval particles from each assumed source location and tracking them forward in time. However, various strategies have been employed for releasing these larval particles: including randomly, consistently, or a number proportional to the location's area or larval production, which causes ambiguous results. We demonstrate, using theoretical arguments and numerical simulations from Lake Whitefish (*Coregonus clupeaformis*) larvae in Lake Erie, that SR depends on larval production at each source location. This dependency suggests that SR may not be computed unambiguously in these models unless realistic larval production is released from all potential source locations. In contrast, parentage analysis studies typically computed SR by assessing the fraction of sampled juveniles that originate locally at a settlement location, instead of identifying larval production at all sources. Therefore, tracking larval particles backward from the settlement location is proposed as a straightforward approach for computing SR. Our findings demonstrate that SR is independent of the number of larval recruits at the settlement location, supporting the employment of backtracking models with randomly released larval particles. In this way, considerable effort and resources, that would otherwise be spent on identifying all potential sources and their larval output, in forward tracking can be saved. We believe this result will have important implications for studies on larval dispersal and recruitment in aquatic systems.

1 Introduction

Most marine species have a pelagic larval phase, during which larvae are transported by currents away from a source population and subsequently recruited into a receiving population, thereby regulating population connectivity (Cowen and

https://doi.org/10.5194/gmd-2024-215
Preprint. Discussion started: 25 March 2025

Geoscientific Model Development Discussions

Sponaugle, 2009; Arevalo et al., 2023; Wood et al., 2014). Since Cowen et al. (2000) stated that marine populations may not be as open as previously thought, there has been accumulating evidence that the probability of dispersal declines rapidly with distance (Almany et al., 2013; Buston and D'aloia, 2013). Furthermore, high values of self-recruitment (SR) and local retention (LR) may be common in many fish populations (Cowen et al., 2000; James et al., 2002; Cowen et al., 2006; Almany et al., 2007; Hamilton et al., 2008; Hogan et al., 2012). This indicates that management decisions, based on open population models, might overestimate larval exchange, potentially leading to mismanagement of both local and downstream populations (Cowen et al., 2000; Nanninga et al., 2015). Therefore, measuring SR and LR is essential for quantifying localized recruitment, assessing the self-replenishment and persistence of populations, and designing effective fisheries management plans (D'aloia et al., 2013; Burgess et al., 2014; Lett et al., 2015).

SR is defined as the fraction of all recruits at a location that originated locally (Botsford et al., 2009); it reflects regional replenishment and the openness to recruitment from other locations (Burgess et al., 2014; Lett et al., 2015). LR indicates the self-persistence of a population, in the absence of external propagule inputs (Burgess et al., 2014). LR has been defined as the ratio of locally produced setters to total local larval release (Botsford et al., 2009) or as the ratio of locally produced settlers to the total number of locally released larvae, that successfully settle in suitable nursery locations and survive (Hogan et al., 2012). Here, we define the latter, which includes only successfully settled larvae, as local retention, while the former, which encompasses both successful and unsuccessful settlers (those settling in unsuitable nursery locations), is termed “theoretical” local retention (TLR), as described by Shi et al. (2024). The three metrics (LR, TLR, and SR) share the same numerator, representing the number of local settlers, but differ in their denominators.

Parentage analysis and/or larval tagging have been widely used to estimate LR, TLR and SR (Jones et al., 1999; Pinsky et al., 2012; D'aloia et al., 2013; Lett et al., 2015; Planes et al., 2009). By assigning sampled juveniles to their parents according to DNA relationships, researchers can identify their source locations and quantify the number of settlers originating from each source location. However, the total number of eggs/larvae produced at a source location i, $N_i^{'}$, and their survival rates remain poorly understood, making it challenging to empirically assess LR and TLR (Lett et al., 2015). Consequently, biophysical models, typically coupled with forward-in-time Lagrangian particle tracking models (herein referred to as forward tracking models), have been widely applied to study larval dispersal and compute TLR and LR (Chaput et al., 2022; Saint-Amand et al., 2023; Sato et al., 2023; Gurdek-Bas et al., 2022). By assuming that N_i larvae are produced at location i, i.e., assuming $N_i^{'} = N_i$, releasing N_i larval particles from i and tracking them forward in time, TLR can be computed as the ratio of the number of larvae that settle at location i to N_i. LR can also be computed by excluding the larvae that settle in unsuitable nursery locations from N_i (Gurdek-Bas et al., 2022). It is worth noting that both LR and TLR at location i are independent of $N_i^{'}$, making it effective to release a random number of larval particles N_i from the location, as will be demonstrated in this research.

Typically, SR has also been computed using biophysical models (Paris et al., 2005; Hiddink et al., 2013; Dubois et al., 2016; Klein et al., 2016; Faillettaz et al., 2018; Lequeux et al., 2018; Meerhoff et al., 2018; Hidalgo et al., 2019; Wolanski et al., 2021; Saint-Amand et al., 2023; Michie et al., 2024; Nadal et al., 2024; Corrochano-Fraile et al., 2022; Sato

https://doi.org/10.5194/gmd-2024-215
Preprint. Discussion started: 25 March 2025


Geoscientific Model Development Discussions

et al., 2023). In this case, a certain number of larval particles are released from each assumed source location and tracked forward in time. SR at the settlement location *j* is then computed as the number of larvae both released from and settled at *j*, divided by the total number of larvae that settled at *j*. Notably, the denominator is related to the larval production from all source locations, which may transport larvae to *j*. In contrast, the numerator, representing the number of settlers originating from *j* itself, varies only with the larval production at *j*. Changes in larval production at any of the source locations can thus potentially alter the total number of settlers at *j*, resulting in variation in SR. However, simply identifying all potential source locations poses a challenge and it remains even less understood how many larval particles should be released from each source location.

At least four distinct strategies have been employed for releasing larval particles. For example, Hiddink et al. (2013), Dubois et al. (2016), and Faillettaz et al. (2018) assumed that larval production was consistent across all source locations, where each location was assumed to produce 500 larvae (Dubois et al., 2016), 1500 larvae (Faillettaz et al., 2018), or 10,000 larvae (Hiddink et al., 2013), respectively. In this strategy, the SR at a location of interest was computed independently of the larval production at each source location. Sato et al. (2023) assumed that 900 larvae were produced from each of the 84 source locations at Puerto Galera (PG) in the Verde Island Passage. The 84 source locations were randomly divided into three regions, with 5 locations at PG, 45 locations east of PG, and 34 locations west of PG. Therefore, 4500 larval particles were released from PG, 40500 from the east and 30600 from the west, resulting in 17.9, 4.4, and 71.9 particles settled at PG, respectively, giving a value of SR at region PG as 17.9 / (17.9 + 4.4 + 71.9) = 0.19. However, if PG was divided into more locations, the number of local settlers at PG (i.e., 17.9) may be increased, altering the value of SR. D'agostini et al. (2015) assumed that larger locations produced proportionally more larvae than smaller ones, and Saint-Amand et al. (2023) assumed a constant density of 500 larvae/km^2 and a minimum release of 100 larvae for the smallest location. The resultant SR at each location, therefore, depended on the location area. Nolasco et al. (2022) assumed larval production at each location was proportional to the product of the adult abundance score by the spawning intensity score. From these examples, it remains uncertain whether larval production at each location is constant or proportional to the area of the location. Accurately releasing the number of larvae produced at each location may yield a more precise estimation of SR; however, the realistic number of larval productions at each location remains a challenge to observe. Additionally, there may be unknown source locations contributing to unexpected recruitment that is not accounted for in these simulations, causing potentially misleading estimates of SR.

Conversely, Shi et al. (2024) used backward-in-time Lagrangian particle tracking models (SWIM-V2.0, herein referred to as backtracking models) to estimate larval hatching locations of Lake Whitefish (*Coregonus clupeaformis*) and proposed that backtracking models may be more efficient in computing SR. Backtracking models, release larval particles from larval sampling locations and track them in reverse time, providing a straightforward approach to modeling recruitment that has been widely applied to study the spawning/hatching locations of fish larvae (Christensen et al., 2007; Thygesen, 2011; Bauer et al., 2014; Gargano et al., 2022; Rowe et al., 2022; Chaput et al., 2023). In this case, the denominator of SR, the total number of settlers at location *j*, $M_j^{'}$ (which is unknown as well), is assumed to be M_j, indicating that M_j larval

https://doi.org/10.5194/gmd-2024-215
Preprint. Discussion started: 25 March 2025

Geoscientific Model Development Discussions

particles will be released from j and tracked backward in time. It is no longer necessary to identify all potential source locations and their corresponding larval production for estimating the denominator. The SR at j is independent of the real number of recruits at j, making it effective to release a random number (M_j) of larval particles from j, as will be demonstrated.

In this research, we show theoretically that in forward tracking simulations, LR and TLR are independent of the larval production from the source location, while SR is not. Moreover, using forward tracking models to compute SR can yield ambiguous results. This assertion brings into question the numerous estimates of SR from studies that have employed different strategies for releasing larval particles from each source location within forward tracking models. Additionally, we compute SR using backtracking models and show that this SR remains independent of the number of recruits at the settlement location. We validate these assertions by applying both forward and backtracking models to compute LR and SR associated with observations of Lake Whitefish (*Coregonus clupeaformis*) larvae sampled in Lake Erie. Our findings are applicable to both freshwater and marine species that undergo a pelagic larval phase.

2 Theoretical Development

2.1 Self-recruitment from forward tracking models

Suppose that there are a set of n locations associated with larval hatching and larval settling or recruitment (locations 1, 2, …, i, j, …, n). Here, $N_i^{'}$ represents the realistic number of eggs spawned or newly hatched larvae at location i. The larvae become pelagic upon hatching and undergo a dispersal process, being transported away from the source location by water currents. The dispersal rate from patch i to patch j, denoted as D_{ij}, is defined as the proportion of larvae released from location i that settle at location j. The theoretical local retention (TLR) at location i, commonly used in forward tracking simulations (Saint-Amand et al., 2023; Sato et al., 2023), is defined as follows, as per Shi et al. (2024):

$$\mathrm{TLR}_i = \frac{D_{ii}N_i^{'}}{N_i^{'}} = D_{ii}\ , \tag{1}$$

At the end of larval dispersal, some larvae settle at suitable nursery locations, while some settle in unsuitable ones; the latter are referred to as ‘unsuccessful’ settlers (Almany et al., 2017). By excluding the unsuccessful settlers from the denominator of TLR, we obtain local retention (LR), which is also known as relative local retention (Hogan et al., 2012; Lett et al., 2015):

$$\mathrm{LR}_i = \frac{D_{ii}N_i^{'}}{\sum_{j=1}^{n} D_{ij}\,N_i^{'}} = \frac{D_{ii}}{\sum_{j=1}^{n} D_{ij}}\ , \tag{2}$$

Self-recruitment (SR), the ratio of local larval recruitment to all the recruitment at the settlement location, at location i is (Botsford et al., 2009; Lett et al., 2015; Almany et al., 2017):

https://doi.org/10.5194/gmd-2024-215
Preprint. Discussion started: 25 March 2025

Geoscientific Model Development Discussions

$$\mathrm{SR}_i = \frac{D_{ii}N_i^{'}}{\sum_{j=1}^{n} D_{ji}N_j^{'}}, \quad (3)$$

Assuming consistent larval production across all locations, i.e., $N_1^{'} = ... = N_i^{'} = N_j^{'} = ... = N_n^{'}$, the SR can be expressed as follows:

$$\mathrm{SR}_i = \frac{D_{ii}}{\sum_{j=1}^{n} D_{ji}}, \quad (4)$$

Here, both TLR and LR are theoretically independent of $N_i^{'}$. When performing the forward tracking simulations, releasing a random number of larval particles, N_i, from the location i, is demonstrated as an effective approach to compute the unambiguous values of TLR and LR. In practice, a sufficiently large number of particles is needed for the dispersal rate (D) to converge and accurately reflect the underlying processes. With more particles, the estimate of D stabilizes as it better captures the full distribution of trajectories. TLR provides a minimum value of LR as stated by Shi et al. (2024), as the denominator contains both successfully and unsuccessfully settlers. However, SR is shown to be dependent on larval production at each source location ($N_1^{'}, N_2^{'}, \ldots, N_i^{'}, N_j^{'}, \ldots, N_n^{'}$), demonstrating that any strategies for larval particle release other than releasing the realistic larval production from each source location in forward tracking may not unambiguously compute SR. Though assuming consistent larval production across all locations can make SR independent of larval production (Eq. 4), this assumption can lead to significant discrepancies in the estimated value of SR compared to using realistic value of larval production (Eq. 3), particularly when there are many source locations.

2.2 Self-recruitment from backward tracking models

An alternate approach is to release larval particles from the locations where larvae are recruited into the population (settlement locations) and track them backward-in-time. Suppose that there are a set of m locations associated with larval hatching and recruitment respectively (locations 1, 2, …, i, j, …, m). $M_i^{'}$ larvae are recruited into settlement location i. The recruitment rate $R_{ij}^{'}$ is defined as the proportion of larvae recruited into the settlement location i that originated from the source location j. SR at location i can be written as:

$$\mathrm{SR}_i = \frac{R_{ii}^{'}M_i^{'}}{M_i^{'}} = R_{ii}^{'}, \quad (5)$$

SR at location i is theoretically equivalent to the recruitment rate at that location, independent of the number of recruits at i. This is reasonable; for instance, in parentage analysis studies, sampling all recruits at a location in the field is often challenging, SR is thus estimated as the number of sampled juveniles assigned to originate locally based on DNA relationships, divided by the total number of sampled juveniles at that location (D'aloia et al., 2013; Almany et al., 2017). This computation of SR, based on sampled recruits, can be used to reflect the overall recruitment dynamics, further supporting the notion that SR is independent of the number of recruits at the location of interest.

https://doi.org/10.5194/gmd-2024-215
Preprint. Discussion started: 25 March 2025

Geoscientific Model Development Discussions

In backtracking simulations, a random number of larval particles M_i are typically released from location *i*. It is important to note that by the end of the simulation, some particles will have settled in suitable hatching or source locations, while some will have settled in unsuitable locations, leading to what is termed 'unreal' recruitment (Shi et al., 2024). The settlement rate R_{ij}, is the ratio of the number of larval particles that settle at location *j* and originate from location *i*, divided by the total number of larval particles released from location *i*. The difference between R_{ij} and $R_{ij}^{'}$ lies in the denominator, which corresponds to M_i and $M_i^{'}$, respectively. Substituting R_{ij} and M_i for $R_{ij}^{'}$ and $M_i^{'}$ in Eq. 5 does not yield SR, but rather the theoretical self-recruitment (TSR), which is the minimum value of SR, as its denominator contains unreal recruits (Shi et al., 2024):

$$\mathrm{TSR}_i = \frac{R_{ii}M_i}{M_i} = R_{ii}\,, \tag{6}$$

The SR at location *i*, in backtracking simulations, is obtained by excluding the unreal recruits from the denominator of TSR, expressed as:

$$\mathrm{SR}_i = \frac{R_{ii}M_i}{\sum_{j=1}^{n} R_{ij}M_i} = \frac{R_{ii}}{\sum_{j=1}^{n} R_{ij}}\,, \tag{7}$$

Unlike Eq. (3), SR at location *i*, computed through backtracking models, is theoretically independent of the number of larval particles released from the location (M_i). This independence arises because the settlement rate remains constant regardless of M_i, as will be demonstrated later with numerical data. Consequently, it is effective to release a random number of particles from the settlement location of interest.

The LR at location *i* in backtracking simulations is:

$$\mathrm{LR}_i = \frac{R_{ii}M_i}{\sum_{j=1}^{n} R_{ji}M_j}\,, \tag{8}$$

The LR, estimated by backtracking, is dependent on M_i, unlike for forward tracking (Eq. 2). Moreover, backtracking cannot be used to compute TLR as there is no unsuccessful dispersal in the simulation, and similarly, forward tracking cannot compute TSR as there is no unreal recruitment.

2.3 Number of larvae produced and recruited at each location

The number of larvae produced at each location $N_i^{'}$ may be computed for use in forward tracking simulations to obtain unbiased estimates of SR, based on the number of recruits to location *i*, $M_i^{'}$.

If M_i particles are released from location *i* in backtracking simulations, $M_i \cdot \sum_{j=1}^{n} R_{ij}$ particles are real recruits, as they settle in suitable hatching locations; correspondingly, $M_i \cdot (1 - \sum_{j=1}^{n} R_{ij})$ are unreal recruits. Therefore, if $M_i^{'}$ recruits are sampled at a location *i*, the number of real recruits $M_i \cdot \sum_{j=1}^{n} R_{ij}$ must equal $M_i^{'}$, and $M_i = M_i^{'} \big/ \sum_{j=1}^{n} R_{ij}$ particles should be

https://doi.org/10.5194/gmd-2024-215
Preprint. Discussion started: 25 March 2025


Geoscientific Model Development Discussions

182 released at the location for backtracking. The number of recruits, at location i, that originates from location j can thus be
183 obtained as:

184 $$N_{ji}^{'} = R_{ij} \cdot M_{i}^{'} \Big/ \sum_{j=1}^{n} R_{ij} \,, \tag{9}$$

185 From the dispersal rate D_{ji}, the number of larvae produced at location j, is:

186 $$N_{j}^{'} = \frac{N_{ji}^{'}}{D_{ji}} = M_{i}^{'} \cdot \frac{R_{ij}}{D_{ji}} \cdot \frac{1}{\sum_{j=1}^{n} R_{ij}} \,, \tag{10}$$

187 Interestingly, if the number of recruits at another location a is $M_{a}^{'}$, then the number of larvae produced at location j can also
188 be written as:

189 $$N_{j}^{'} = M_{a}^{'} \cdot \frac{R_{aj}}{D_{ja}} \cdot \frac{1}{\sum_{j=1}^{n} R_{aj}} \,, \tag{11}$$

190 Combining Eq. (10) and (11), we can obtain the number of recruits at location a as:

191 $$M_{a}^{'} = M_{i}^{'} \cdot \frac{R_{ij}}{D_{ji}} \cdot \frac{D_{ja}}{R_{aj}} \cdot \sum_{j=1}^{n} \frac{R_{aj}}{R_{ij}} \,, \tag{12}$$

192 Both $N_{j}^{'}$ and $M_{a}^{'}$ are undefined when the dispersal, recruitment or settlement rates become zero.

193 **3 Putting Theory into Practice: Application to Lake Erie**

194 **3.1 Study area**

195 Shi et al. (2024) identified the Lake Whitefish larval hatching locations in Lake Erie from backtracking simulations. The
196 locations were primarily distributed along the western and southern flanks of the western basin. Considering that Lake
197 Whitefish eggs incubate on hard substrates (Amidon et al., 2021), we selected four regions with hard substrates along the
198 western and southern flanks of the western basin as potential hatching locations (Fig. 1). These were the release regions for
199 larval particles in our forward tracking simulations. We refer to these locations as the Detroit River Mouth (region A),
200 Western Shoreline (region B), Midlake Reefs (region C), and Bass Islands (region D). The Midlake Reef and Bass Island
201 regions were also selected as settlement regions, where we released larval particles for backtracking simulations.

https://doi.org/10.5194/gmd-2024-215
Preprint. Discussion started: 25 March 2025

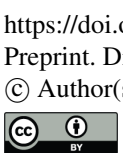

Geoscientific Model Development Discussions

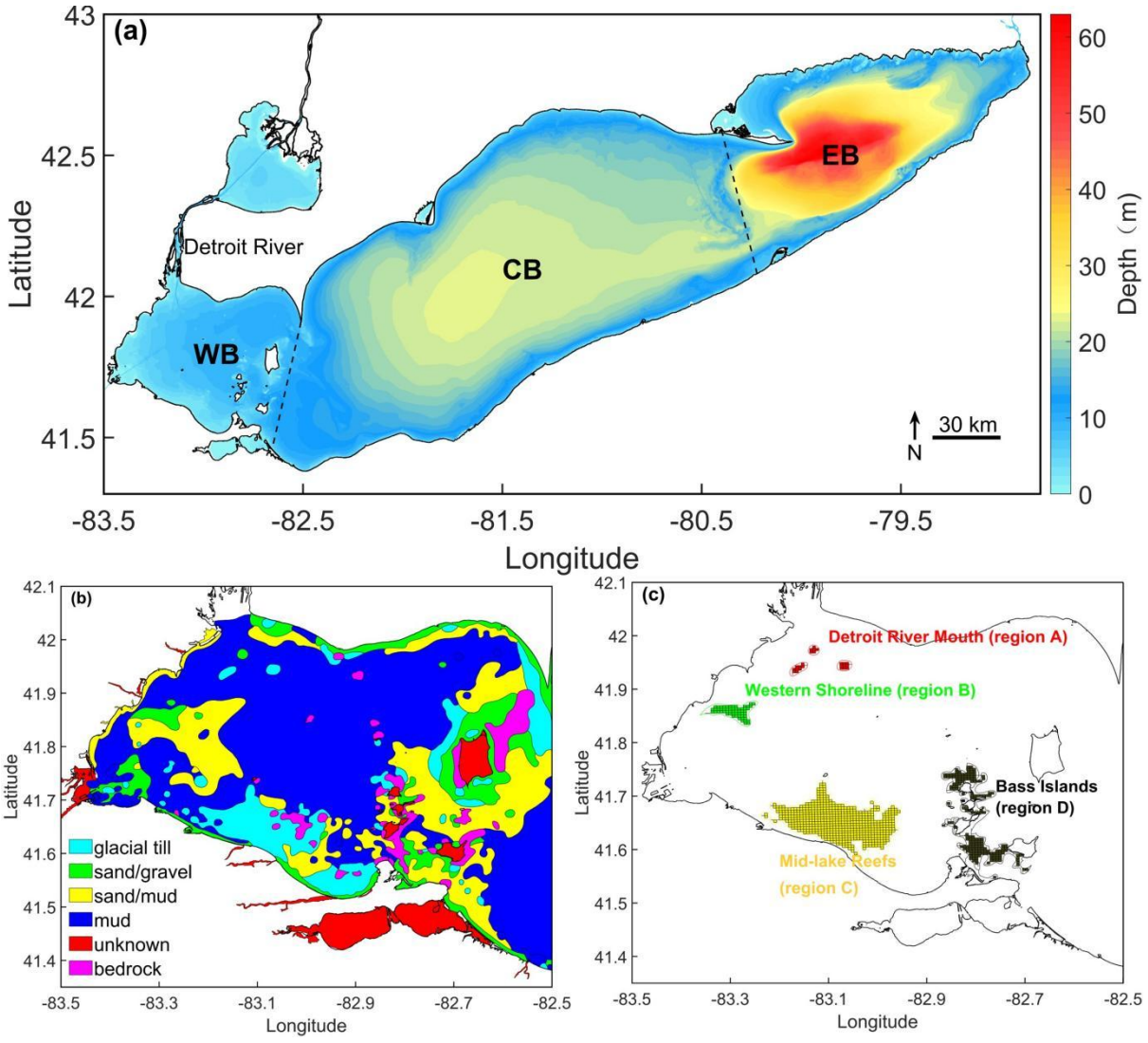

Figure 1: (a) Map showing the three basins of Lake Erie: western basin (WB), central basin (CB), and eastern basin (EB). The lake bathymetry was obtained from https://www.ngdc.noaa.gov/mgg/greatlakes/erie.html. (b) Substrate distributions in the western basin from side-scan sonar transects (Haltuch et al., 2000). (c) Color coded Lake Whitefish (*Coregonus clupeaformis*) hatching locations (Detroit River Mouth in red, region A; Western Shoreline in green, region B; Mid-Lake Reefs in yellow, region C; Bass Islands in black, region D), where larval particles were released at the centre of each 500 m × 500 m AEM3D grid (black cross-hatching).

3.2 The hydrodynamic model

Larval particles were transported using output from an application of the hydrostatic 3D Reynolds-averaged Navier-Stokes equation model, the Aquatic Ecosystem Model (AEM3D) (www.hydronumerics.com.au). The model simulated the water temperature and currents in Lake Erie during a continuous 2017-2019 hindcast run, using a 500 m × 500 m horizontal grid with 45 vertical layers (Shi et al., 2024; Lin et al., 2022). There was fine resolution (0.5 m) through the surface layer, metalimnion and bottom of the central basin, and coarser resolution layers (5 m) through the hypolimnion of the deeper

https://doi.org/10.5194/gmd-2024-215
Preprint. Discussion started: 25 March 2025


Geoscientific Model Development Discussions

eastern basin. The model was forced with surface meteorological data (wind speed and direction, air temperature, relative humidity and long- and short-wave solar radiation) from four weather stations, had five inflows (Detroit, Maumee, Sandusky, Cuyahoga and Grand rivers) and the Niagara River outflow. Model calibration and validation were described in the supplemental material (tables S2-S4) of Shi et al. (2024).

The AEM3D model, and its non-parallel predecessor the Estuary and Lake Computer Model (ELCOM), have been applied to Lake Erie to backtrack the present Lake Whitefish larval observations and determine hatching locations (Shi et al., 2024); to hindcast the thermal structure (León et al., 2005), internal wave dynamics (Valipour et al., 2015), surface wave / sediment transport (Lin et al., 2021), nutrient and chlorophyll-a distributions (Leon et al., 2011), seasonal succession of phytoplankton groups (Wang et al., 2024); and to forecast storm surge and upwelling/downwelling events (Lin et al., 2022).

3.3 The Lagrangian particle tracking model

We used a Matlab®-based Lagrangian particle tracking model (SWIM-v2.0) to study SR. An earlier version of this model was applied forward-in-time to track silver eel (*Anguilla rostrata* and *Anguilla anguilla*) migration (Béguer-Pon et al., 2016) and backward-in-time to determine the larval Lake Whitefish hatching locations used in this study (Shi et al., 2024). Diel vertical migration and active swimming behavior were not considered (Di Stefano et al., 2022; Rowe et al., 2022; Suca et al., 2022).

A horizontal turbulent diffusivity K_h = 0.1 m^2s^{-1} and timestep dt_p = 600 s were used in both forward and backward tracking simulations and larval particles were released at a 3-m water depth and were removed if they encountered the lake boundary (Shi et al., 2024). In the forward tracking simulations, particles were released daily at 12:00-noon between 21 March and 8 May 2018 (in four regions; Table A1, regions A, B, C and D) and were tracked for 12 days. In the backtracking simulations, particles were released daily at 12:00-noon between 2 April and 20 May 2018 (in two regions for 12 days; Table A1, regions C and D). Each release region was divided into 500 m × 500 m AEM3D grid cells, and particles were released at the centres of these cells.

3.4 Nomenclature and data analysis

In forward tracking, the number of larval particles released from location i was N_i and the number of particles released from location i that settled at location j was F_{ij}. For example, if N_A particles were released from region A; F_{AC} represents the number of particles that settled in region C that were released from region A. In backtracking, the number of particles released from location i was M_i and the number of particles released from location i that settled at location j was B_{ij}. For example, if M_C particles were released from region C; B_{CA} represents the number of particles that settled in location A that were released from region C.

The dispersal rate D_{ij} and settlement rate R_{ij} are given by:

$$D_{ij} = F_{ij}/N_i\,, \tag{13}$$

https://doi.org/10.5194/gmd-2024-215
Preprint. Discussion started: 25 March 2025

Geoscientific Model Development Discussions

$$R_{ij}=B_{ij}/M_i\ , \tag{14}$$

When computed from forward and backward simulations, local retention and self-recruitment are written as LR_F, LR_B, SR_F and SR_B, respectively. From Eqs. (11) and (14), the number of larvae produced at each location $N_i^{'}$ is:

$$N_i^{'} = B_{ji}/D_{ij}\ , \tag{15}$$

For example, $N_A^{'}$ is the number of larvae produced from region A. To estimate $N_i^{'}$, from Eq. (11), requires both backward and forward tracking simulations, and the number of recruits to the location. Here, we only backtracked particles from region C and D; therefore, $N_i^{'}$ can be computed as B_{Ci}/D_{iC} or B_{Di}/D_{iD}, which are referred to as $N_{i\_C}^{'}$ and $N_{i\_D}^{'}$, respectively. Dividing $N_{A\_C}^{'}$ by the number of AEM3D grid cells in region A (or the total area of the 500 m × 500 m grid cells) gives the density $d_{A\_C}^{'}$.

4 Results

As examples of forward and backward trajectories, and to illustrate the validity of the tracking simulations, we show backtracked larval particles from the Midlake Reefs (region C, Fig. 2a) and forward tracked particles from the Western Shoreline (region B, Fig. 2b). When particles were released from region C and tracked backward for a period of 12 days, they mostly settled along the southern and western franks of the western basin (yellow dots in Fig. 2a), consistent with the settlement distributions in Shi et al. (2024). Most particles were backtracked to regions westward of the release locations with few travelling to regions eastward, following the predominant west-to-east flow patterns of water movement in the lake (Beletsky et al., 2013).

When particles were released from region B and tracked forward for a period of 12 days, they were mostly transported to the east of the release locations (green dots in Fig. 2b), also consistent with the flow patterns moving particles from west to east in the lake. However, some of the particles were transported southeast and northeast of the release locations, which seems to be counter-intuitive but is not unreasonable given the complex topography and variability in the wind direction in the region. Adding the northeast release region to the backtracking simulations would, therefore, lead to backward trajectories to region B.

https://doi.org/10.5194/gmd-2024-215
Preprint. Discussion started: 25 March 2025

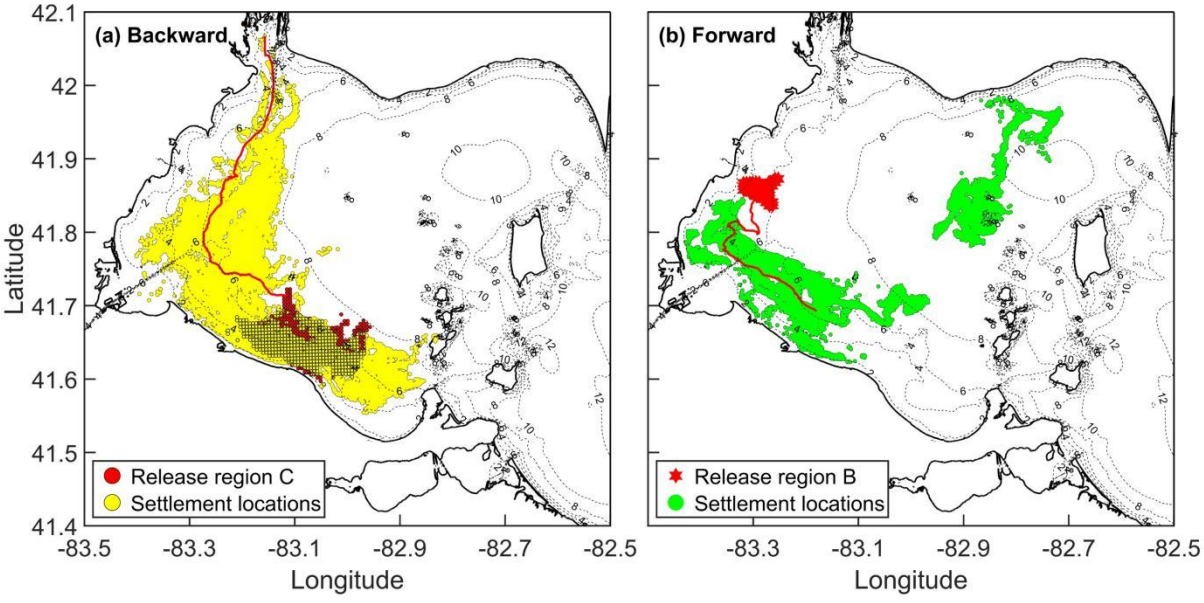

Figure 2: The settlement location distributions when (a) releasing particles from the red circles and tracking them backward, (b) releasing particles from the red stars and tracking them forward. Yellow circles indicate the settlement locations in backtracking and green circles indicate the settlement locations in forward tracking. Red lines show particle trajectories.

In the forward tracking simulations, the number of settled larval particles (F_{ij}) varied with the number of particles released (N_i) and the dispersal rate (D_{ij}) was independent of N_i (Table 1). Both TLR and LR had negligible variation with N_i, for example TLR_F at region C equaled to D_{CC} as ~ 0.13 and TLR_F at region D equaled to D_{DD} as ~ 0.024. Based on Eq. 3, LR_F equaled to 0 for region A and region B, ~ 0.755 for region C, and ~ 0.99 for region D.

The individual SR_F values are not given in Table 1, because there were 81 different SRs obtained at region C through changing N_i, consistent with Eq. (3), ranging from 0.22 to 0.95. For example, when 151200 particles were released from A, 140000 particles from B, 19460 from C and 148400 from D, the SR_F at region C was $2537/(4668+4195+2537+37)=0.22$; whereas when 16800 particles, 17500 particles, 155680 particles, and 18550 particles were released from region A, B, C, and D respectively, SR_F at region C was $20758/(527+501+20758+2)=0.95$. In other words, releasing more particles from region C and fewer particles from the other regions increased the SR at region C, as D_{CC} was much larger than D_{AC}, D_{BC} and D_{DC}. Indeed, SR can approach 1 or 0 through adjustment of N_i. The true value of SR can only be obtained if the actual number of larvae produced at each location is released (i.e., $N_i = N_i^{'}$); however, $N_i^{'}$ remains unknown.

If all four regions released the same number of particles, SR_F would be only a function of D_{ij}, and would be independent of N_i. For example, the SR_F for region C was $D_{CC}/D_{AC}+D_{BC}+D_{CC}+D_{DC}= 0.68$ and the SR_F for region D was $D_{DD}/D_{AD}+D_{BD}+D_{CD}+D_{DD}= 0.32$.

https://doi.org/10.5194/gmd-2024-215
Preprint. Discussion started: 25 March 2025

Geoscientific Model Development Discussions

In the backtracking simulations, the number of settled larval particles B_{ij} varied with M_i. The settlement rate R_{ij} and SR_B had negligible variation with M_i (Table 2); showing the SR calculated from backtracking to be independent of M_i, as indicated by Eq. (7). The correct SR values from backtracking may be compared to the erroneous ones from forward tracking, which had assumed N_i to be the same for all sources. SR_B at region C was larger than SR_F (0.97 vs. 0.68) and SR_B at region D was smaller (0.18 vs. 0.32) because of the variation in the number of particles released from each location N_i. If the recruits to region C, $M_C^{'}$, was equal to $M_C \cdot (R_{CA} + R_{CB} + R_{CC} + R_{CD})$, then the number of particles that should have been released in forward tracking from region C should be ~ 2 times greater than those from region D, ~ 10 times greater than those from region B, and ~ 50 times greater than those from region A (see $N_{A\_C}^{'}$, $N_{B\_C}^{'}$, $N_{C\_C}^{'}$, and $N_{D\_C}^{'}$ in Table 3); assuming the same $N_i^{'}$ increased the denominator of SR_F at region C, and decreased the denominator of SR_F at region D. When scaled by the number of cells in each region, the larval density from region C was roughly half that from region D, ~4 times that from region B, and ~10 times that from region A (see $d_{A\_C}^{'}$, $d_{B\_C}^{'}$, $d_{C\_C}^{'}$, and $d_{D\_C}^{'}$ in Table 3).

Table 1. Number of particles released from the four regions $\boldsymbol{N_i}$, settled to four regions $\boldsymbol{F_{ij}}$, and the dispersal rate $\boldsymbol{D_{ij}}$ in the forward tracking simulations. The regions are the Detroit River Mouth (region A), Western Shoreline (region B), Midlake Reefs (region C), and Bass Islands (region D).

$\boldsymbol{N_A}$	$\boldsymbol{F_{AA}}$	$\boldsymbol{F_{AB}}$	$\boldsymbol{F_{AC}}$	$\boldsymbol{F_{AD}}$	$\boldsymbol{D_{AA}}$	$\boldsymbol{D_{AB}}$	$\boldsymbol{D_{AC}}$	$\boldsymbol{D_{AD}}$	$\boldsymbol{LR\_F_A}$
16800	0	0	527	140	0	0	0.0313	0.0083	0
84000	0	0	2587	665	0	0	0.0308	0.0079	0
151200	0	0	4668	1189	0	0	0.0309	0.0079	0
$\boldsymbol{N_B}$	$\boldsymbol{F_{BA}}$	$\boldsymbol{F_{BB}}$	$\boldsymbol{F_{BC}}$	$\boldsymbol{F_{BD}}$	$\boldsymbol{D_{BA}}$	$\boldsymbol{D_{BB}}$	$\boldsymbol{D_{BC}}$	$\boldsymbol{D_{BD}}$	$\boldsymbol{LR\_F_B}$
17500	0	0	501	0	0	0	0.029	0	0
70000	0	0	2097	0	0	0	0.030	0	0
140000	0	0	4195	0	0	0	0.030	0	0
$\boldsymbol{N_C}$	$\boldsymbol{F_{CA}}$	$\boldsymbol{F_{CB}}$	$\boldsymbol{F_{CC}}$	$\boldsymbol{F_{CD}}$	$\boldsymbol{D_{CA}}$	$\boldsymbol{D_{CB}}$	$\boldsymbol{D_{CC}}$	$\boldsymbol{D_{CD}}$	$\boldsymbol{LR\_F_C}$
19460	0	0	2537	843	0	0	0.130	0.0433	0.751
77840	0	0	10440	3327	0	0	0.134	0.0427	0.758
155680	0	0	20758	6739	0	0	0.133	0.0433	0.755
$\boldsymbol{N_D}$	$\boldsymbol{F_{DA}}$	$\boldsymbol{F_{DB}}$	$\boldsymbol{F_{DC}}$	$\boldsymbol{F_{DD}}$	$\boldsymbol{D_{DA}}$	$\boldsymbol{D_{DB}}$	$\boldsymbol{D_{DC}}$	$\boldsymbol{D_{DD}}$	$\boldsymbol{LR\_F_D}$
18550	0	0	2	435	0	0	0.0001	0.0235	0.995
74200	0	0	19	1800	0	0	0.0002	0.0242	0.990
148400	0	0	37	3648	0	0	0.0002	0.0246	0.990

https://doi.org/10.5194/gmd-2024-215
Preprint. Discussion started: 25 March 2025

Geoscientific Model Development Discussions

Table 2. Number of particles released from two regions $\boldsymbol{M_i}$ and settled in four regions $\boldsymbol{B_{ij}}$, settlement rate $\boldsymbol{R_{ij}}$, and self-recruitment from the backtracking simulations. The regions are the Detroit River Mouth (region A), Western Shoreline (region B), Midlake Reefs (region C), and Bass Islands (region D).

$\boldsymbol{M_C}$	$\boldsymbol{B_{CA}}$	$\boldsymbol{B_{CB}}$	$\boldsymbol{B_{CC}}$	$\boldsymbol{B_{CD}}$	$\boldsymbol{R_{CA}}$	$\boldsymbol{R_{CB}}$	$\boldsymbol{R_{CC}}$	$\boldsymbol{R_{CD}}$	$\boldsymbol{SR\_B_C}$
19460	17	94	3778	2	8.7×10^{-4}	0.0048	0.194	0.0001	0.971
77840	75	337	15300	8	9.6×10^{-4}	0.0043	0.196	0.0001	0.973
155680	137	685	30659	22	8.8×10^{-4}	0.0044	0.197	0.0001	0.973
$\boldsymbol{M_D}$	$\boldsymbol{B_{DA}}$	$\boldsymbol{B_{DB}}$	$\boldsymbol{B_{DC}}$	$\boldsymbol{B_{DD}}$	$\boldsymbol{R_{DA}}$	$\boldsymbol{R_{DB}}$	$\boldsymbol{R_{DC}}$	$\boldsymbol{R_{DD}}$	$\boldsymbol{SR\_B_D}$
18550	0	0	1911	407	0	0	0.103	0.022	0.176
74200	0	0	7628	1718	0	0	0.102	0.023	0.184
148400	1	0	15302	3430	6.7×10^{-6}	0	0.103	0.023	0.183

Table 3. The number of larvae and larval density (No. per cell) produced in the four regions. The regions are the Detroit River Mouth (region A), Western Shoreline (region B), Midlake Reefs (region C), and Bass Islands (region D).

$\boldsymbol{M_C}$	$\boldsymbol{N'_{A\_C}}$	$\boldsymbol{N'_{B\_C}}$	$\boldsymbol{N'_{C\_C}}$	$\boldsymbol{N'_{D\_C}}$	$\boldsymbol{d'_{A\_C}}$	$\boldsymbol{d'_{B\_C}}$	$\boldsymbol{d'_{C\_C}}$	$\boldsymbol{d'_{D\_C}}$
19460	550	3133	28406	10000	22.9	62.7	51.1	94.3
77840	2427	11233	115038	40000	101.1	224.7	206.9	377.4
155680	4434	22833	230519	110000	184.8	456.7	414.6	1037.7
$\boldsymbol{M_D}$	$\boldsymbol{N'_{A\_D}}$	$\boldsymbol{N'_{B\_D}}$	$\boldsymbol{N'_{C\_D}}$	$\boldsymbol{N'_{D\_D}}$	$\boldsymbol{d'_{A\_D}}$	$\boldsymbol{d'_{B\_D}}$	$\boldsymbol{d'_{C\_D}}$	$\boldsymbol{d'_{D\_D}}$
18550	0	0	44134	16545	0	0	79.4	156.1
74200	0	0	176166	69837	0	0	316.8	658.8
148400	126	0	353395	139431	5.3	0	635.6	1315.4

5 Discussion

We have shown, using both theoretical arguments and numerical data, that self-recruitment (SR) cannot be unambiguously computed using forward Lagrangian particle tracking models. In contrast, backward Lagrangian particle tracking models have demonstrated to be straightforward and effective in calculating SR.

SR depends on the larval production at each source location (Eq. 3), as noted by Lett et al. (2015). This dependence suggests that using forward tracking models to compute SR may be invalid if any strategy for larval particle release, such as releasing a random number, an equal number, or a number proportional to the area of the location, is employed, rather than releasing the realistic larval production from each source location. Our numerical data confirmed that variations in the release of larval particles from any source location can lead to different values of SR. This is in addition to the likelihood that there are unknown source locations contributing unexpected recruitment that are not accounted for in the simulation.

https://doi.org/10.5194/gmd-2024-215
Preprint. Discussion started: 25 March 2025


Geoscientific Model Development Discussions

Similarly, researchers do not need to measure the larval production and dispersal rates of every potential source location to estimate the SR at a given location. Instead, they can easily obtain the SR by estimating the number of local juveniles from the total sampled juveniles at a given location, based on DNA relationships (D'aloia et al., 2013; Almany et al., 2017).

This shows that SR is independent of the number of larval recruits at the location of interest. This independence makes it effective to compute SR using backward tracking models by releasing a random number of larval particles from the location, as our numerical data demonstrated that SR had negligible variations with the number of larval particles released from the settlement location. Despite the increasing usage of backtracking models to estimate larval hatching/spawning locations and to study larval recruitment, few studies have used backtracking models to compute SR (Torrado et al., 2021). Considering the limitations of backtracking models, for example that they are diffusive backward-in-time rather than being convergent, comparisons with results from parentage analysis should be undertaken to further verify the validity of SR when computed using backtracking models.

Local retention (LR) is typically more challenging to evaluate empirically, compared to SR, as sampling the eggs/larvae that successfully grow into juveniles is more difficult than sampling recruits/juveniles (Lett et al., 2015). While parentage analysis can identify the source of sampled juveniles, accurately accounting for the total number of juveniles originating from a given source remains a challenge, as some juveniles are inevitably transported to unknown locations and may be missed. For example, Almany et al. (2017) sampled adult and juvenile *Amphiprion percula* and *Chaetodon vagabundus* from eight different locations in Papua New Guinea and assigned juveniles to their parents according to DNA relationships. The location of their parents served as the source location of the juveniles, allowing the researchers to determine the number of juveniles produced from each source location. However, the total number of larvae produced (including those lost to mortality) remained unknown. The difficulty in sampling newly hatched larvae, i.e., measuring $N_i^{'}$, is likely why it is common to apply different larval particle release strategies from each source location in forward tracking simulations.

Knowing the number of recruits $M_i^{'}$, or the larval production $N_i^{'}$ at one location, can allow us to estimate the number of recruits and larval production at all other locations from Eqs. (11) and (12) using forward and backward tracking simulations. An approach to estimate $N_i^{'}$ was proposed (Eq. 10), based on the number of recruits at a settlement location $M_j^{'}$, the settlement rate R_{ji} and the dispersal rate D_{ij}. From Eqs. (10) and (11), the $N_i^{'}$ values can be computed based on the recruits at different settlement locations and should be consistent. For example, $N_i^{'}$ computed from the recruits at regions C and D should be equal, such that $N_{i\_C}^{'} = N_{i\_D}^{'}$. However, large differences between $N_{i\_C}^{'}$ and $N_{i\_D}^{'}$ were modeled (Table 3). When D_{ij} or R_{ji} approaches zero, the computation of $N_i^{'}$ is undefined (section 2.3), which partly explains the difference. Moreover, random numbers of recruits M_j were released from regions C and D, which also caused differences between $N_{i\_C}^{'}$ and $N_{i\_D}^{'}$. These differences can be reconciled when D_{ij} and R_{ji} are non-zero by adjusting M_D based on M_C; $N_{i\_C}^{'}$ would then equal $N_{i\_D}^{'}$. For example, if $M_C = 19460$ particles released and backtracked from region C, the realistic number of recruits at region C is $M_C^{'} = M_C \cdot (R_{CA} + R_{CB} + R_{CC} + R_{CD}) = 3887$, the realistic recruits at region D, $M_D^{'}$=1514 would then be

https://doi.org/10.5194/gmd-2024-215
Preprint. Discussion started: 25 March 2025

Geoscientific Model Development Discussions

estimated based on Eq. (12). The particles released and backtracked from region D should, therefore, be $M_D = M_D^{'}/R_{DA}+R_{DB}+R_{DC}+R_{DD} = 12112$ instead of 18550 in Table 3. The $N_C^{'}$ value based on the recruits at region C, $N_{C\_C}^{'}$, would be equal to 28820 (from Eq. 11) and $N_C^{'}$ estimated from the recruits to region D, $N_{C\_D}^{'}$, would equal to 28811. The negligible difference between 28820 and 28811 indicates the correctness of Eqs. (11) and (12).

6 Conclusions

Our findings show that self-recruitment (SR) is dependent on larval production at each potential source location that may transport larvae to the location of interest. From this, we show theoretically and confirm using Lake Whitefish simulations, that SR may not be computed unambiguously in forward tracking models without first identifying all the potential source locations and their respective larval production. The latter becomes particularly evident given that four different strategies for releasing larval particles from each source location have been employed. In contrast, in parentage analysis studies, it is typically not necessary to measure the larval production and dispersal rates of every potential source location to estimate SR at a given settlement location. Instead, by directly identifying the proportion of locally originating juveniles among the sampled juveniles at a given location based on DNA relationships, SR can be determined more efficiently and accurately. Similarly, releasing larval particles at the settlement location and tracking them backward in time offers a straightforward approach to computing SR. Our findings demonstrated that SR is independent of the number of larval recruits at the settlement location, making it viable to release a random number of larval particles. SR can thus be easily obtained as the fraction of larval particles that settle locally, saving considerable effort and resources that would otherwise be spent identifying all potential sources and their larval output. Furthermore, we proposed an approach to estimate larval production at each source location by leveraging the connectivity between source and settlement locations, computed through combining forward and backward tracking models. When run in isolation, backtracking models are only able to compute SR (or theoretical SR) and the settlement rate, and forward tracking models are only able to compute LR (or theoretical LR) and the dispersal rate. Whereas using a combination of both models allows for the calculation of not only SR and LR, but also the larval production at each source location and the number of recruits at settlement locations. The ability to accurately compute these metrics will significantly improve understanding of population connectivity. The findings were validated using numerical data for the Lake Whitefish freshwater species but are also appliable to marine species with a pelagic larval phase.

https://doi.org/10.5194/gmd-2024-215
Preprint. Discussion started: 25 March 2025

Geoscientific Model Development Discussions

Appendix A

Table A1. Release regions, times and durations for forward and backward tracking simulations.

	Release regions	Release times	Tracking periods (day)	Number of cells
Forward	Detroit River Mouth (Region A)	21 March to 8 May	12	24
	Western Shoreline (Region B)	21 March to 8 May	12	50
	Midlake Reefs (Region C)	21 March to 8 May	12	556
	Bass Islands (Region D)	21 March to 8 May	12	106
Backward	Midlake Reefs (Region C)	2 April to 20 May	12	556
	Bass Islands (Region D)	2 April to 20 May	12	106

Table A2. The description of the notations in this research.

Notation	Description
B_{ij}	Number of particles recruited to site j that were released from site i in backtracking
$d_i^{'}$	Number of larvae per cell (500 m × 500 m) produced from site i
$d_{i\_j}^{'}$	Number of larvae per cell (500 m × 500 m) produced from site i estimated based on the recruits to site j
D_{ij}	Proportion of larvae released from site i that recruit into the juvenile population at site j
F_{ij}	Number of particles recruited to site j that were released from site i in forward tracking
LR_i	Ratio of local larval recruitment at site i to the number of larvae released locally, that settled in suitable nursery sites
M_i	Number of particles released from site i in the backtracking simulations
$M_i^{'}$	Number of larval recruits to site i
N_i	Number of particles released from site i in forward tracking simulations
$N_i^{'}$	Number of larvae produced at site i
$N_{i\_j}^{'}$	Number of larvae produced from site i estimated from the recruits to site j
$N_{ji}^{'}$	Number of recruits at site i that were released from site j
R_{ij}	Proportion of particles released from patch i that settled in patch j in the backtracking simulations
SR_i	Ratio of local larval recruitment at site i to all recruitment at site i
TLR_i	Ratio of local larval recruitment to site i to local larvae released

https://doi.org/10.5194/gmd-2024-215
Preprint. Discussion started: 25 March 2025

Geoscientific Model Development Discussions

TSR_i	Ratio of particles that settled at site i to all the particles released from site i in backtracking simulations

Code and data availability. The AEM3D executable was used as a black-box hydrodynamic transport code. The AEM3D source code was not modified in this application but is available with permission from HydroNumerics. The model setup for AEM3D are available at https://doi.org/10.5281/zenodo.14749408. The forward and backward particle tracking models were performed in Matlab. Their code and simulated date are all available at https://doi.org/10.5281/zenodo.14789098. The velocity output from AEM3D is also presented at https://doi.org/10.5281/zenodo.14789098.

Author contributions. WS conceived the main study design, developed the theory, performed the simulations and analyses. WS wrote the first draft of manuscript and LB and JDA revised the draft significantly. LB and SLS co-supervised the research and provided resources. JDA, LB, SLS and YMZ acquired research funding. All authors contributed to the project conceptualization, and editing and revising the manuscript.

Competing interests. The contact author has declared that none of the authors has any competing interests.

Disclaimer. Publisher's note: Copernicus Publications remains neutral with regard to jurisdictional claims in published maps and institutional affiliations.

Financial support. This work was supported by the Ontario Ministry of Natural Resources and Forestry, the Canada Ontario Agreement program and an NSERC Alliance Grant program to Josef D. Ackerman, Leon Boegman, and Shiliang Shan.

References

Almany, G. R., Berumen, M. L., Thorrold, S. R., Planes, S., and Jones, G. P.: Local replenishment of coral reef fish populations in a marine reserve, Science, 316, 742-744, 2007.

Almany, G. R., Hamilton, R. J., Bode, M., Matawai, M., Potuku, T., Saenz-Agudelo, P., Planes, S., Berumen, M. L., Rhodes, K. L., Thorrold, S. R., Russ, G. R., and Jones, G. P.: Dispersal of grouper larvae drives local resource sharing in a coral reef fishery, Curr Biol, 23, 626-630, 10.1016/j.cub.2013.03.006, 2013.

Almany, G. R., Planes, S., Thorrold, S. R., Berumen, M. L., Bode, M., Saenz-Agudelo, P., Bonin, M. C., Frisch, A. J., Harrison, H. B., Messmer, V., Nanninga, G. B., Priest, M. A., Srinivasan, M., Sinclair-Taylor, T., Williamson, D. H., and Jones, G. P.: Larval fish dispersal in a coral-reef seascape, Nat Ecol Evol, 1, 148, 10.1038/s41559-017-0148, 2017.

https://doi.org/10.5194/gmd-2024-215
Preprint. Discussion started: 25 March 2025

411 Amidon, Z. J., DeBruyne, R. L., Roseman, E. F., and Mayer, C. M.: Contemporary and Historic Dynamics of Lake
412 Whitefish (Coregonus clupeaformis) Eggs, Larvae, and Juveniles Suggest Recruitment Bottleneck during First Growing
413 Season, Annales Zoologici Fennici, 58, 10.5735/086.058.0405, 2021.
414 Arevalo, E., Cabral, H. N., Villeneuve, B., Possémé, C., and Lepage, M.: Fish larvae dynamics in temperate estuaries: A
415 review on processes, patterns and factors that determine recruitment, Fish and Fisheries, 24, 466-487, 10.1111/faf.12740,
416 2023.
417 Bauer, R. K., Gräwe, U., Stepputtis, D., Zimmermann, C., and Hammer, C.: Identifying the location and importance of
418 spawning sites of Western Baltic herring using a particle backtracking model, ICES Journal of Marine Science, 71, 499-509,
419 10.1093/icesjms/fst163, 2014.
420 Béguer-Pon, M., Shan, S., Thompson, K. R., Castonguay, M., Sheng, J., and Dodson, J. J.: Exploring the role of the physical
421 marine environment in silver eel migrations using a biophysical particle tracking model, ICES Journal of Marine Science, 73,
422 57-74, 10.1093/icesjms/fsv169, 2016.
423 Beletsky, D., Hawley, N., and Rao, Y. R.: Modeling summer circulation and thermal structure of Lake Erie, Journal of
424 Geophysical Research: Oceans, 118, 6238-6252, 10.1002/2013jc008854, 2013.
425 Botsford, L. W., White, J. W., Coffroth, M. A., Paris, C. B., Planes, S., Shearer, T. L., Thorrold, S. R., and Jones, G. P.:
426 Connectivity and resilience of coral reef metapopulations in marine protected areas: matching empirical efforts to predictive
427 needs, Coral Reefs, 28, 327-337, 10.1007/s00338-009-0466-z, 2009.
428 Burgess, S. C., Nickols, K. J., Griesemer, C. D., Barnett, L. A., Dedrick, A. G., Satterthwaite, E. V., Yamane, L., Morgan, S.
429 G., White, J. W., and Botsford, L. W.: Beyond connectivity: how empirical methods can quantify population persistence to
430 improve marine protected-area design, Ecol Appl, 24, 257-270, 10.1890/13-0710.1, 2014.
431 Buston, P. M. and D'Aloia, C. C.: Marine ecology: reaping the benefits of local dispersal, Curr Biol, 23, R351-353,
432 10.1016/j.cub.2013.03.056, 2013.
433 Chaput, R., Quigley, C. N., Weppe, S. B., Jeffs, A. G., de Souza, J., and Gardner, J. P. A.: Identifying the source populations
434 supplying a vital economic marine species for the New Zealand aquaculture industry, Sci Rep, 13, 9344, 10.1038/s41598-
435 023-36224-y, 2023.
436 Chaput, R., Sochala, P., Miron, P., Kourafalou, V. H., Iskandarani, M., and Kaplan, D. M.: Quantitative uncertainty
437 estimation in biophysical models of fish larval connectivity in the Florida Keys, ICES Journal of Marine Science, 79, 609-
438 632, 10.1093/icesjms/fsac021, 2022.
439 Christensen, A., Daewel, U., Jensen, H., Mosegaard, H., St John, M., and Schrum, C.: Hydrodynamic backtracking of fish
440 larvae by individual-based modelling, Marine Ecology Progress Series, 347, 221-232, 10.3354/meps06980, 2007.
441 Corrochano-Fraile, A., Adams, T. P., Aleynik, D., Bekaert, M., and Carboni, S.: Predictive biophysical models of bivalve
442 larvae dispersal in Scotland, Frontiers in Marine Science, 9, 10.3389/fmars.2022.985748, 2022.
443 Cowen, R. K. and Sponaugle, S.: Larval dispersal and marine population connectivity, Ann Rev Mar Sci, 1, 443-466,
444 10.1146/annurev.marine.010908.163757, 2009.

https://doi.org/10.5194/gmd-2024-215
Preprint. Discussion started: 25 March 2025

445 Cowen, R. K., Paris, C. B., and Srinivasan, A.: Scaling of Connectivity in Marine Populations, Science, 311, 522-527, 2006.
446 Cowen, R. K., Lwiza, K. M. M., Sponaugle, S., Paris, C. B., and Olson, D. B.: Connectivity of marine populations: open or
447 closed, Science, 287, 857-859, 2000.
448 D'Aloia, C. C., Bogdanowicz, S. M., Majoris, J. E., Harrison, R. G., and Buston, P. M.: Self-recruitment in a Caribbean reef
449 fish: a method for approximating dispersal kernels accounting for seascape, Mol Ecol, 22, 2563-2572, 10.1111/mec.12274,
450 2013.
451 D'Agostini, A., Gherardi, D. F. M., and Pezzi, L. P.: Connectivity of Marine Protected Areas and Its Relation with Total
452 Kinetic Energy, Plos One, 10, 10.1371/journal.pone.0139601, 2015.
453 Di Stefano, M., Legrand, T., Di Franco, A., Nerini, D., and Rossi, V.: Insights into the spatio-temporal variability of
454 spawning in a territorial coastal fish by combining observations, modelling and literature review, Fisheries Oceanography,
455 32, 70-90, 10.1111/fog.12609, 2022.
456 Dubois, M., Rossi, V., Ser-Giacomi, E., Arnaud-Haond, S., López, C., and Hernández-García, E.: Linking basin-scale
457 connectivity, oceanography and population dynamics for the conservation and management of marine ecosystems, Global
458 Ecology and Biogeography, 25, 503-515, 10.1111/geb.12431, 2016.
459 Faillettaz, R., Paris, C. B., and Irisson, J.-O.: Larval Fish Swimming Behavior Alters Dispersal Patterns From Marine
460 Protected Areas in the North-Western Mediterranean Sea, Frontiers in Marine Science, 5, 10.3389/fmars.2018.00097, 2018.
461 Gargano, F., Garofalo, G., Quattrocchi, F., and Fiorentino, F.: Where do recruits come from? Backward Lagrangian
462 simulation for the deep water rose shrimps in the Central Mediterranean Sea, Fisheries Oceanography, 31, 369-383,
463 10.1111/fog.12582, 2022.
464 Gurdek-Bas, R., Benthuysen, J. A., Harrison, H. B., Zenger, K. R., and van Herwerden, L.: The El Nino Southern Oscillation
465 drives multidirectional inter-reef larval connectivity in the Great Barrier Reef, Sci Rep, 12, 21290, 10.1038/s41598-022-
466 25629-w, 2022.
467 Hamilton, S. L., Regetz, J., and Warner, R. R.: Postsettlement survival linked to larval life in a marine fish., Proc Natl Acad
468 Sci U S A, 105, 1561-1566, 2008.
469 Hidalgo, M., Rossi, V., Monroy, P., Ser-Giacomi, E., Hernandez-Garcia, E., Guijarro, B., Massuti, E., Alemany, F., Jadaud,
470 A., Perez, J. L., and Reglero, P.: Accounting for ocean connectivity and hydroclimate in fish recruitment fluctuations within
471 transboundary metapopulations, Ecol Appl, 29, e01913, 10.1002/eap.1913, 2019.
472 Hiddink, J. G., Andrello, M., Mouillot, D., Beuvier, J., Albouy, C., Thuiller, W., and Manel, S.: Low Connectivity between
473 Mediterranean Marine Protected Areas: A Biophysical Modeling Approach for the Dusky Grouper Epinephelus marginatus,
474 PLoS ONE, 8, 10.1371/journal.pone.0068564, 2013.
475 Hogan, J. D., Thiessen, R. J., Sale, P. F., and Heath, D. D.: Local retention, dispersal and fluctuating connectivity among
476 populations of a coral reef fish, Oecologia, 168, 61-71, 10.1007/s00442-011-2058-1, 2012.
477 James, M. K., Armsworth, P. R., Mason, L. B., and Bode, L.: The structure of reef fish metapopulations: modelling larval
478 dispersal and retention patterns, Proc Biol Sci, 269, 2079-2086, 10.1098/rspb.2002.2128, 2002.

https://doi.org/10.5194/gmd-2024-215
Preprint. Discussion started: 25 March 2025


Geoscientific Model Development Discussions

Jones, G. P., Milicich, M. J., Emslie, M. J., and Lunow, C.: Self-recruitment in a coral reef fish population, Nature, 402, 802-804, 1999.

Klein, M., Teixeira, S., Assis, J., Serrão, E. A., Gonçalves, E. J., and Borges, R.: High Interannual Variability in Connectivity and Genetic Pool of a Temperate Clingfish Matches Oceanographic Transport Predictions, Plos One, 11, 10.1371/journal.pone.0165881, 2016.

Leon, L. F., Smith, R. E. H., Hipsey, M. R., Bocaniov, S. A., Higgins, S. N., Hecky, R. E., Antenucci, J. P., Imberger, J. A., and Guildford, S. J.: Application of a 3D hydrodynamic–biological model for seasonal and spatial dynamics of water quality and phytoplankton in Lake Erie, Journal of Great Lakes Research, 37, 41-53, 10.1016/j.jglr.2010.12.007, 2011.

León, L. F., Imberger, J., Smith, R. E. H., Hecky, R. E., Lam, D. C. L., and Schertzer, W. M.: Modeling as a tool for nutrient management in Lake Erie: a hydrodynamics study, Journal of Great Lakes Research, 31, 309-318 2005.

Lequeux, B. D., Ahumada-Sempoal, M. A., Lopez-Perez, A., and Reyes-Hernandez, C.: Coral connectivity between equatorial eastern Pacific marine protected areas: A biophysical modeling approach, PLoS One, 13, e0202995, 10.1371/journal.pone.0202995, 2018.

Lett, C., Nguyen-Huu, T., Cuif, M., Saenz-Agudelo, P., and Kaplan, D. M.: Linking local retention, self-recruitment, and persistence in marine metapopulations, Ecology, 96, 2236-2244, 10.1890/14-1305.1, 2015.

Lin, S. Q., Boegman, L., Shan, S. L., and Mulligan, R.: An automatic lake-model application using near-real-time data forcing: development of an operational forecast workflow (COASTLINES) for Lake Erie, Geoscientific Model Development, 15, 1331-1353, 10.5194/gmd-15-1331-2022, 2022.

Lin, S. Q., Boegman, L., Valipour, R., Bouffard, D., Ackerman, J. D., and Zhao, Y.: Three-dimensional modeling of sediment resuspension in a large shallow lake, Journal of Great Lakes Research, 47, 970-984, 10.1016/j.jglr.2021.04.014, 2021.

Meerhoff, E., Yannicelli, B., Dewitte, B., Díaz-Cabrera, E., Vega-Retter, C., Ramos, M., Bravo, L., Concha, E., Hernández-Vaca, F., and Véliz, D.: Asymmetric connectivity of the lobster Panulirus pascuensis in remote islands of the southern Pacific: importance for its management and conservation, Bulletin of Marine Science, 94, 753-774, 10.5343/bms.2017.1114, 2018.

Michie, C., Lundquist, C. J., Lavery, S. D., and Della Penna, A.: Spatial and temporal variation in the predicted dispersal of marine larvae around coastal Aotearoa New Zealand, Frontiers in Marine Science, 10, 10.3389/fmars.2023.1292081, 2024.

Nadal, I., Picciulin, M., Falcieri, F. M., García-Lafuente, J., Sammartino, S., and Ghezzo, M.: Spatio-temporal connectivity and dispersal seasonal patterns in the Adriatic Sea using a retention clock approach, Frontiers in Marine Science, 11, 10.3389/fmars.2024.1360077, 2024.

Nanninga, G. B., Saenz-Agudelo, P., Zhan, P., Hoteit, I., and Berumen, M. L.: Not finding Nemo: limited reef-scale retention in a coral reef fish, Coral Reefs, 34, 383-392, 10.1007/s00338-015-1266-2, 2015.

Nolasco, R., Dubert, J., Acuña, J. L., Aguión, A., Cruz, T., Fernandes, J. N., Geiger, K. J., Jacinto, D., Macho, G., Mateus, D., Rivera, A., Román, S., Thiébaut, E., Vazquez, E., and Queiroga, H.: Biophysical modelling of larval dispersal and

https://doi.org/10.5194/gmd-2024-215
Preprint. Discussion started: 25 March 2025


Geoscientific Model Development Discussions

population connectivity of a stalked barnacle: implications for fishery governance, Marine Ecology Progress Series, 694, 105-123, 10.3354/meps14097, 2022.

Paris, C. B., Cowen, R. k., Claro, R., and Lindeman, K. C.: Larval transport pathways from Cuban snapper (Lutjanidae) spawning aggregations based on biophysical modeling, Marine Ecology Progress Series, 296, 93-106, 2005.

Pinsky, M. L., Palumbi, S. R., Andrefouet, S., and Purkis, S. J.: Open and closed seascapes: where does habitat patchiness create populations with high fractions of self-recruitment?, Ecol Appl, 22, 1257-1267, 10.1890/11-1240.1, 2012.

Planes, S., Jones, G. P., and Thorrold, S. R.: Larval dispersal connects fish populations in a network of marine protected areas, Proc Natl Acad Sci U S A, 106, 5693-5697, 2009.

Rowe, M. D., Prendergast, S. E., Alofs, K. M., Bunnell, D. B., Rutherford, E. S., and Anderson, E. J.: Predicting larval alewife transport in Lake Michigan using hydrodynamic and Lagrangian particle dispersion models, Limnology and Oceanography, 67, 2042-2058, 10.1002/lno.12186, 2022.

Saint-Amand, A., Lambrechts, J., and Hanert, E.: Biophysical models resolution affects coral connectivity estimates, Sci Rep, 13, 9414, 10.1038/s41598-023-36158-5, 2023.

Sato, M., Honda, K., Nakamura, Y., Bernardo, L. P. C., Bolisay, K. O., Yamamoto, T., Herrera, E. C., Nakajima, Y., Lian, C., Uy, W. H., Fortes, M. D., Nadaoka, K., and Nakaoka, M.: Hydrodynamics rather than type of coastline shapes self-recruitment in anemonefishes, Limnology and Oceanography, 10.1002/lno.12399, 2023.

Shi, W., Boegman, L., Shan, S., Zhao, Y., Ackerman, J. D., Amidon, Z., Jabbari, A., and Roseman, E.: A Larval "Recruitment Kernel" to Predict Hatching Locations and Quantify Recruitment Patterns, Water Resources Research, 60, 10.1029/2023wr036099, 2024.

Suca, J. J., Ji, R., Baumann, H., Pham, K., Silva, T. L., Wiley, D. N., Feng, Z., and Llopiz, J. K.: Larval transport pathways from three prominent sand lance habitats in the Gulf of Maine, Fisheries Oceanography, 31, 333-352, 10.1111/fog.12580, 2022.

Thygesen, U. H.: How to reverse time in stochastic particle tracking models, Journal of Marine Systems, 88, 159-168, 10.1016/j.jmarsys.2011.03.009, 2011.

Torrado, H., Mourre, B., Raventos, N., Carreras, C., Tintoré, J., Pascual, M., and Macpherson, E.: Impact of individual early life traits in larval dispersal: A multispecies approach using backtracking models, Progress in Oceanography, 192, 10.1016/j.pocean.2021.102518, 2021.

Valipour, R., Bouffard, D., Boegman, L., and Rao, Y. R.: Near-inertial waves in Lake Erie, Limnology and Oceanography, 60, 1522-1535, 10.1002/lno.10114, 2015.

Wang, Q., Boegman, L., Nakhaei, N., and Ackerman, J. D.: Multi-year three-dimensional simulation of seasonal variation in phytoplankton species composition in a large shallow lake, Ocean Modelling, 189, 10.1016/j.ocemod.2024.102374, 2024.

Wolanski, E., Richmond, R. H., and Golbuu, Y.: Oceanographic chaos and its role in larval self-recruitment and connectivity among fish populations in Micronesia, Estuarine, Coastal and Shelf Science, 259, 10.1016/j.ecss.2021.107461, 2021.

https://doi.org/10.5194/gmd-2024-215
Preprint. Discussion started: 25 March 2025

546 Wood, S., Paris, C. B., Ridgwell, A., and Hendy, E. J.: Modelling dispersal and connectivity of broadcast spawning corals at
547 the global scale, Global Ecology and Biogeography, 23, 1-11, 10.1111/geb.12101, 2014.
548